

# Kinetic and Spectroscopic Characterization of Fluorescent Ribose-Modified ATP Analogs upon Interaction with Skeletal Muscle Myosin Subfragment 1<sup>†</sup>

Paul B. Conibear, Daren S. Jeffreys, Charnjit K. Seehra, Robert J. Eaton, and Clive R. Bagshaw\*

Department of Biochemistry, University of Leicester, Leicester LE1 7RH, U.K.

Received August 7, 1995; Revised Manuscript Received November 17, 1995<sup>®</sup>

**ABSTRACT:** The interaction of the fluorescent ATP analog 2'(3')-O-[N-[2-[3-(5-fluoresceinyl)thioureido]ethyl]carbamoyl]adenosine 5'-triphosphate (FEDA-ATP) with rabbit skeletal myosin subfragment 1 (S1) and acto-S1 was studied. This and related ATP analogs are potentially useful for determination of the ATPase activity of single myosin filaments using fluorescence microscopy [Sowerby et al. (1993) *J. Mol. Biol.* 234, 114–123]. However, it is necessary that such analogs mimic ATP in their kinetics of turnover. The apparent second-order association rate constants for FEDA-ATP binding to S1 and for FEDA-ATP-induced dissociation of acto-S1 are about 4 times slower than those for ATP. As with ATP, the hydrolysis step is fast, so that the M•FEDA-ADP•P<sub>i</sub> complex is the major steady-state intermediate. The turnover rate is the same for the 2' and 3' FEDA-ATP derivatives and similar to that of ATP itself. The dissociation rate constant for FEDA-ADP from S1 is identical to that for ADP. Actin-activated turnover is comparable for both FEDA-ATP and ATP. The corresponding rhodamine and sulfoindocyanine, Cy3.18 (Cy3), derivatives also appear to be reasonable analogs. FEDA-ATP binding leads to a 25–40% reduction in fluorescein fluorescence. Spectral properties of the bound nucleotide were explored by trapping FEDA-ADP as its aluminum fluoride complex. The fluorescence quenching is a consequence of a reduction in both absorbance and excited-state lifetime, but there is little change in spectral shape.

The elucidation of the myosin and actomyosin ATPase pathways by transient kinetic methods has made extensive use of fluorescence methodology, including the development of fluorescent ATP derivatives whose spectral properties are resolved from the intrinsic tryptophan fluorescence (Yount, 1975; Trentham et al., 1976). Given the requirement that these compounds should be good ATP analogs, their design has been based largely on the principle of minimum possible modification to the ATP structure. Early studies focused on modification of the adenine ring and resulted in probes which could be excited at 300–320 nm, such as formycin triphosphate (Bagshaw et al., 1972) and 1-*N*<sup>6</sup>-ethenoadenosine triphosphate (Garland & Cheung, 1979). More recently, a series of analogs has been developed by derivatization of the 2' and 3' ribose hydroxyl groups, of which mant-ATP<sup>1</sup> (Hiratsuka, 1983) has proven to be a particularly useful probe for the actomyosin system (Woodward et al., 1991). In fact, early studies showed that myosin was fairly tolerant to modification of the ribose moiety (Tonomura et al., 1967). The reason for this is now clearly evident from the crystal

structures of nucleotide complexes of S1 (Fisher et al., 1995). ATP binds in an anti conformation with the phosphate and adenosine moieties embedded in the active-site pocket, while the 2' and 3' ribose hydroxyls face outward to the solvent.

Recently, there has been increasing interest in the development of *in vitro* motility assays where the nature of mechanochemical coupling is experimentally tractable. Thus, with immobilization of myosin molecules on a surface, it is possible to follow translocation of and force developed on single actin filaments under the light microscope (Kron & Spudich, 1986; Kishino & Yanagida, 1988; Finer et al., 1994). However, uncertainty remains over the ATP turnover accompanying these events (Harada et al., 1990; Uyeda et al., 1990; Burton, 1992). It is desirable to be able to measure ATP turnover by the filaments under observation in the *in vitro* motility assay (involving less than 1 zmol of myosin), a feat which requires a fluorescence microscopy approach (Conibear et al., 1995). To date, measurements of the actin-activated ATPase have been restricted to estimates of steady-state phosphate production from picomolar amounts of myosin (Hayashi et al., 1989; Harada et al., 1990; Kron et al., 1991). However, progress has been made in using fluorescent ATP analogs to follow the ATPase of myosin, in the absence of actin (Sowerby et al., 1993; Funatsu et al., 1995a), and provides the basis for further advances.

mant-ATP ( $\lambda_{\text{ex}} = 356 \text{ nm}$ ,  $\lambda_{\text{em}} = 450 \text{ nm}$ ) itself can be detected using standard ultrafluar objective lenses, but the sensitivity is poor and the background signal is high because of the low transmission and luminescence of such lenses in the UV region (Bagshaw et al., 1992). We therefore synthesized a fluorescein derivative of ATP (FEDA-ATP) and the corresponding rhodamine and Cy-3 derivatives (REDA-ATP and Cy3-EDA-ATP respectively) which, in

<sup>†</sup> This work was supported by the Wellcome Trust and an MRC Studentship (D.S.J.). Instrumentation was purchased through grants from the SERC (now BBSRC) and MRC.

\* To whom correspondence should be addressed: Dr. C. R. Bagshaw, Department of Biochemistry, University of Leicester, Leicester LE1 7RH, U.K. Telephone: +44 116 252 3545. Fax: +44 116 252 3369. E-mail: crb5@le.ac.uk.

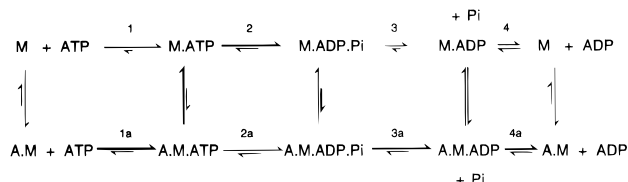
<sup>®</sup> Abstract published in *Advance ACS Abstracts*, February 1, 1996.

<sup>1</sup> Abbreviations: Cy3, sulfoindocyanine dye, Cy3.18; DEDA-nucleotides, 2'(3')-O-[N-[2-[[[5-(dimethylamino)naphthyl]sulfonyl]amino]ethyl]carbamoyl] nucleotides; EDA-ATP, 2'(3')-O-[(aminoethyl)carbamoyl]adenosine 5'-triphosphate; FEDA-ATP, 2'(3')-O-[N-[2-[3-(5-fluoresceinyl)thioureido]ethyl]carbamoyl]adenosine 5'-triphosphate; mant-ATP, 2'(3')-O-(*N*-methylanthraniloyl)-ATP; NTP, nucleoside triphosphate; REDA-ATP, 2'(3')-O-[N-[2-[3-[5(6)-tetraethylrhodamine]thioureido]ethyl]carbamoyl]adenosine 5'-triphosphate; S1, myosin subfragment 1.

contrast, are excited and emit in the visible region (Sowerby et al., 1993). In these derivatives, the fluorophores are linked to the 2' or 3' ribose hydroxyl groups via an ethylenediamine chain. However, apart from the optimization of the optical properties of an analog, it is important to determine the effect of the derivatization of ATP on the kinetic mechanism of the myosin and actomyosin ATPase activity. Stopped-flow studies indicated that the turnover rate of FEDA-ATP with rabbit skeletal myosin S1 was comparable to that of ATP itself, although the observed association rate constants were slower (Sowerby et al., 1993). Here we extend the kinetic and spectroscopic characterization of these analogs in solution.

A minimal scheme for the turnover of ATP by S1 (M) and its activation by actin (A) is given as

Scheme 1



For S1 alone, ATP binding and hydrolysis (steps 1 and 2) are rapid while the rate-limiting step is phosphate ( $P_i$ ) release or, more properly, a preceding isomerization controlling  $P_i$  release (both condensed to step 3). Subsequently, ADP is released with a rate constant ( $k_{+4}$ ) which is an order of magnitude greater than that of the rate-limiting step. Actin binds tightly to myosin in the absence of nucleotide ( $A \cdot M$ ) but is rapidly dissociated after binding ATP. At low actin concentrations, hydrolysis occurs while the proteins are largely dissociated while actin effects activation by rebinding to the product complex and accelerating product release. It is important that any analog used to mimic ATP in motility assays shows the same basic mechanism with rate constants which are comparable to those of ATP itself.

## MATERIALS AND METHODS

**Protein Preparation.** Rabbit skeletal myosin was prepared by a simplified version of the method described by Margossian and Lowey (1982). S1 was prepared from rabbit skeletal myosin using  $\alpha$ -chymotryptic digestion (Weeds & Taylor, 1975). Myosin was stored in 50% glycerol at  $-20^\circ\text{C}$ . S1 was stored at  $-70^\circ\text{C}$  after rapid freezing in liquid nitrogen. Proteolytic enzymes were purchased from Sigma Chemical Co. (Poole, U.K.). General reagents were obtained from Fisons (Loughborough, U.K.).

**Fluorescent Nucleotide Synthesis.** Fluorescent probes were developed on the basis of the strategy of Cremo et al. (1990) for the synthesis of DEDA-nucleotides. FEDA-ATP was prepared by reaction of fluorescein 5-isothiocyanate with EDA-ATP as described previously (Sowerby et al., 1993). Small scale separation of the 2'-O and 3'-O isomers of FEDA-ATP was achieved on a SAX column (Synchropak Q 300A) using a Gilson high-performance liquid chromatography (HPLC) system and isocratic elution with 0.6 M ammonium dihydrogen phosphate at pH 4.0 plus 20% methanol.

REDA-ATP was prepared by reaction of EDA-ATP with rhodamine B isothiocyanate [mixed 5(6) isomers, Sigma Chemical Co.] under the same conditions as for the FEDA-

ATP preparation. It was purified by ion-exchange chromatography on DEAE-Sephadex as described for FEDA-ATP (Sowerby et al., 1993). Cy3-EDA-ATP was prepared similarly but on a smaller scale and without a column purification step. One vial (77 nmol) of the succinimidyl ester of Cy3 (FluoroLink Cy3, monofunctional dye, Biological Detection Systems, Cambridge BioScience, U.K.) was reacted with 154 nmol of EDA-ATP for 2 h at  $20^\circ\text{C}$  in 0.55 mL of 40 mM triethylamine bicarbonate at pH 7.5. Reactions with the Cy3-EDA-ATP preparation were studied with a myosin concentration which exceeded the total nucleotide concentration.

Concentrations of FEDA-nucleotides were based on an  $A_{490} = 78\,000\text{ M}^{-1}\text{ cm}^{-1}$  for the fluorescein dianion predominant at pH  $>8.0$  (Diehl & Horchak-Morris, 1987). Concentrations of REDA-nucleotides were based on  $A_{552} = 106\,000\text{ M}^{-1}\text{ cm}^{-1}$  (Hinckley et al., 1986). Concentrations of Cy3 were based on the starting amount supplied by the manufacturer. Analogs were stored frozen in aqueous solution at  $-20^\circ\text{C}$  and showed no significant breakdown over several months as judged by the amplitude of the quench in fluorescein emission when reacted with a molar excess of S1.

**Kinetic and Spectroscopic Measurements.** Absorption (UV-visible) spectra were recorded using either a Pye Unicam SP8-100 or a Kontron Uvikon 930 spectrophotometer. Fluorescence spectra and slow time courses were measured using a Baird-Atomic SFR100 or a SLM 48000S spectrofluorometer. The latter instrument was equipped with a phase modulation accessory which permitted fluorescence lifetime measurements (Lakowicz, 1983; Ellis et al., 1995). Rapid fluorescence measurements were performed using a SF17MV stopped-flow apparatus (Applied Photophysics, Leatherhead, U.K.). Tryptophan fluorescence was excited at 295 nm and the emission monitored after passage through a 335 nm long-pass filter. Fluorescein fluorescence was excited at either 436 or 495 nm, depending on whether the source was a Hg-Xe or Xe arc lamp, respectively, and the emission monitored using a monochromator setting of 520 nm or a 520 nm long-pass filter. Rhodamine was excited at 546 nm (Hg-Xe lamp) or 560 nm (Xe lamp) and the emission monitored at 590 nm or with a 580 nm long-pass filter. Cy3 fluorescence was excited at 552 nm with a Xe arc and the emission monitored with a 580 nm long-pass filter. Light scattering was measured at  $90^\circ$  with incident light of 320–350 nm.

Quenched-flow measurements were carried out using a custom-built apparatus constructed using the design of Eccleston et al. (1985). The ram was driven by a linear motor (model 15D-351-A8-04, Industrial Devices Co., Norvato, CA) and the movement monitored using a linear potentiometer. Aging times were calculated from the flow velocity, delay times, and known tube diameters and lengths.

Note that stopped-flow concentrations are given as reaction chamber concentrations unless stated otherwise. Stopped-flow transients shown are averages of three to ten individual data, depending on the signal-to-noise ratio of the raw data.

## RESULTS

**Interaction of Fluorescent ATP Analogs with S1.** Addition of S1 to FEDA-ATP results in a quench in fluorescein

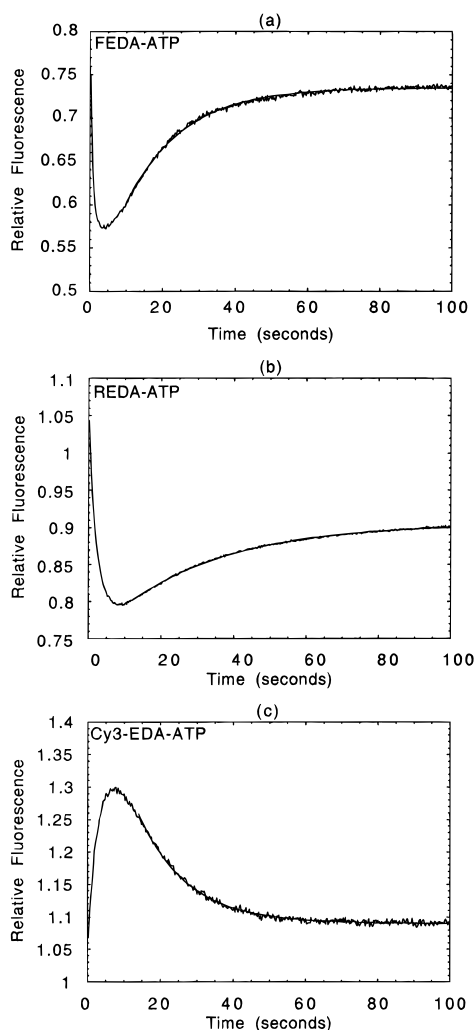


FIGURE 1: Fluorescence transients observed upon addition of nucleotide analogs to S1 under single-turnover conditions in the stopped-flow apparatus. Buffer conditions were as follows: 40 mM NaCl, 20 mM Tris, 1 mM  $\text{MgCl}_2$ , and pH 7.5 at 20 °C. Fluorescence is normalized to that measured for the free ATP analog alone. Zero time is the time at which the flow stops (as is the case with all stopped-flow traces shown). In a, 5  $\mu\text{M}$  S1 was mixed with 1  $\mu\text{M}$  FEDA-ATP. The line superimposed is the least-mean-squares fit of the underlying points to a single exponential which gave  $k = 0.06 \text{ s}^{-1}$ . At the end of the first phase, fluorescence is quenched by 28% relative to the FEDA-ATP alone. After recovery, the quench decreases to 13%. In b, 5  $\mu\text{M}$  S1 was mixed with 0.11  $\mu\text{M}$  REDA-ATP and the data are fitted as in a to give  $k = 0.03 \text{ s}^{-1}$ . At the end of first phase, fluorescence is quenched by 43% and the final quench is 28%. In c, 5  $\mu\text{M}$  S1 was mixed with 1  $\mu\text{M}$  Cy3-EDA-ATP. The data are fitted as above to give  $k = 0.03 \text{ s}^{-1}$ . The fluorescence is enhanced initially by 30% and then recovers to a final enhancement of 7%.

fluorescence as observed in a stopped-flow experiment (Figure 1a). Under single-turnover conditions (i.e.  $[\text{S1}] > [\text{FEDA-ATP}]$ ), there is an immediate recovery in fluorescence with a rate constant of  $0.06 \text{ s}^{-1}$ . This value is similar to the  $k_{\text{cat}}$  for ATP itself, measured in a parallel experiment using tryptophan fluorescence. The change in fluorescence accompanying the formation of intermediate states is best studied under these single-turnover conditions, so as to minimize the contribution from free FEDA-nucleotide. Typically, the minimum fluorescence observed corresponds to a quench of 25–35% of the fluorescence of the FEDA-ATP alone. The final fluorescence value was quenched by about 10–20%, indicating that a significant amount of

FEDA-ADP remained bound to the S1. Increasing the S1 concentration from 5 to 10  $\mu\text{M}$  had little effect on the end point signal, showing that the  $K_d$  for FEDA-ADP binding was  $<5 \mu\text{M}$  and thus most of the FEDA-ADP remained bound under these conditions. Under multiple-turnover conditions (i.e.  $[\text{FEDA-ATP}] > [\text{S1}]$ ), the fluorescein fluorescence remains at a quenched level during the steady state but recovers when the FEDA-ATP is exhausted. However, only a limited molar excess ( $\leq 10$ -fold) of FEDA-ATP can be used in such experiments; otherwise, the observed quench becomes negligible relative to the background signal.

When examined under similar single-turnover conditions, REDA-ATP yields a similar fluorescence profile with an initial quench of 35–45% (Figure 1b). However, the relative amplitude of the recovery phase is less so that the final state is quenched by as much as 25–30%. The REDA-ATP turnover rate constant ( $0.03 \text{ s}^{-1}$ ) was only slightly slower than that for FEDA-ATP. By contrast, Cy3-EDA-ATP shows an initial enhancement of fluorescence by about 30% with a subsequent recovery which is almost complete (Figure 1c). However, the turnover rate for this analog is only slightly slower than for FEDA-ATP and very similar to that of REDA-ATP ( $0.03 \text{ s}^{-1}$ ). A potential problem with this experiment is that any unreacted Cy3 might attack exposed amine groups on S1. However, the result shows no sign of this occurring on the time scale investigated. For the more detailed studies described below, attention is focused mainly on FEDA-ATP since this analog was available in larger amounts than the corresponding rhodamine and Cy3 analogs. Also, FEDA-ATP is more readily purified from EDA-ATP compared to the other analogs which is an important factor in some of the following experiments.

**Association of FEDA-ATP with S1.** The binding of FEDA-ATP to S1 was studied under pseudo-first-order conditions with  $[\text{FEDA-ATP}] > [\text{S1}]$ . The nucleotide-to-protein ratio was kept at 10 as a compromise between achieving strictly first-order kinetics and maintaining a measurable fluorescence change relative to the background signal. FEDA-ATP binding resulted in a quench in both tryptophan and fluorescein fluorescence (Figure 2a,b). The time courses of quenching in fluorescein and tryptophan fluorescence were identical in successive pushes of the stopped-flow apparatus. Both were fitted to single exponentials. At FEDA-ATP concentrations of  $>30 \mu\text{M}$ , there was an indication of saturation of the pseudo-first-order rate constant. The dependence on nucleotide concentration fitted well to a hyperbola with a maximum rate constant of about  $23 \text{ s}^{-1}$ . In a parallel experiment using ATP and monitoring protein tryptophan fluorescence, a maximum observed rate constant of  $46 \text{ s}^{-1}$  was obtained, although the concentration dependence deviated significantly from a hyperbola. These data must delineate a step (or steps) subsequent to NTP binding and are discussed further in this respect below. The apparent second-order rate constant, given as the initial slope of these plots (Figure 2c), is 4-fold lower than that for ATP ( $0.5 \times 10^6 \text{ M}^{-1} \text{ s}^{-1}$  for FEDA-ATP compared to  $2.1 \times 10^6 \text{ M}^{-1} \text{ s}^{-1}$  for ATP).

It was not possible to investigate very high FEDA-ATP concentrations, as has been achieved in studies of other analogs, because of the dominating signal from the free FEDA-ATP and an increasing innerfilter effect. Unfortunately, acrylamide, which has been used as a selective

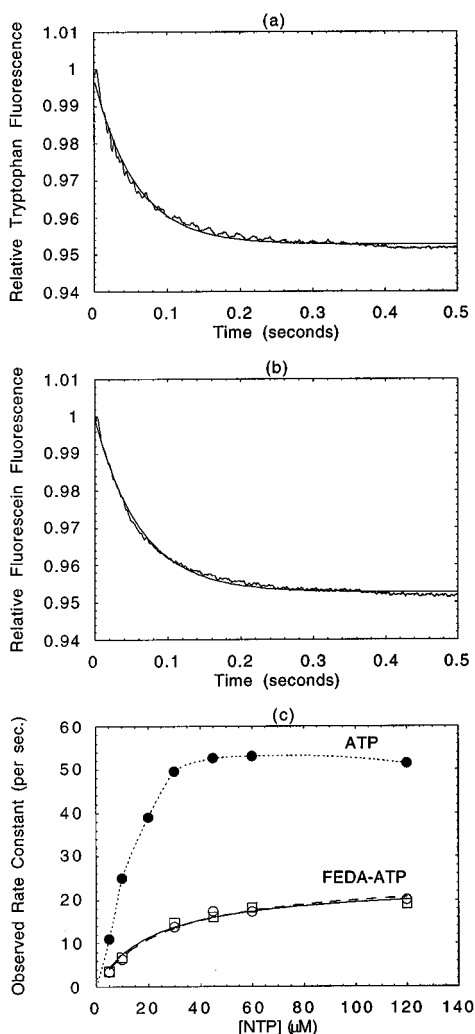


FIGURE 2: (a and b) Fluorescence transients observed upon addition of excess FEDA-ATP ( $45 \mu\text{M}$ ) to S1 ( $4.5 \mu\text{M}$ ) in the stopped-flow apparatus. Buffer conditions were as for Figure 1. Fluorescence is plotted normalized to the value at the beginning of the reaction. The lines superimposed are least-mean-squares fits to single exponentials. In a, the reaction is monitored by tryptophan fluorescence;  $k = 17.4 \text{ s}^{-1}$  with a fluorescence quench of 5.5%. In b, the reaction is monitored by fluorescein fluorescence;  $k = 16.1 \text{ s}^{-1}$ . Part c shows the dependence of the fitted rate constants upon the concentration of nucleotide fitted to a hyperbolic function ( $\circ$ , values for tryptophan fluorescence; and  $\square$ , values for fluorescein fluorescence) and yielded a  $k_{\text{max}}$  of  $23 \text{ s}^{-1}$ . The data obtained in the parallel experiment monitoring tryptophan enhancement with ATP are also shown ( $\bullet$ ) with an interpolated line.  $[\text{NTP}]:[\text{S1}] = 10$  for all data points.

quencher of free nucleotide in the case of 1- $N^6$ -ethenoadenosine triphosphate (Rosenfeld & Taylor, 1984), does not quench the free FEDA-ATP fluorescence so the signal-to-noise could not be improved by this strategy. While 200 mM potassium iodide quenched the fluorescence of FEDA-ATP by a factor of 2, there was little selectivity for the free nucleotide and thus there was no gain in discrimination of the bound state. Neither could energy transfer from tryptophan be used to selectively excite the bound analog, as was possible with mant-ATP (Woodward et al., 1991).

**Turnover of FEDA-ATP Isomers.** Nucleotides modified through the ribose hydroxyl groups usually exist as mixtures of 2' and 3' positional isomers which may undergo slow exchange reactions. In the case of mant-ADP and DEDA-ADP, the 3' isomer predominates in a ratio of about 2:1 around neutral pH (Cremo et al., 1990). Previously, we

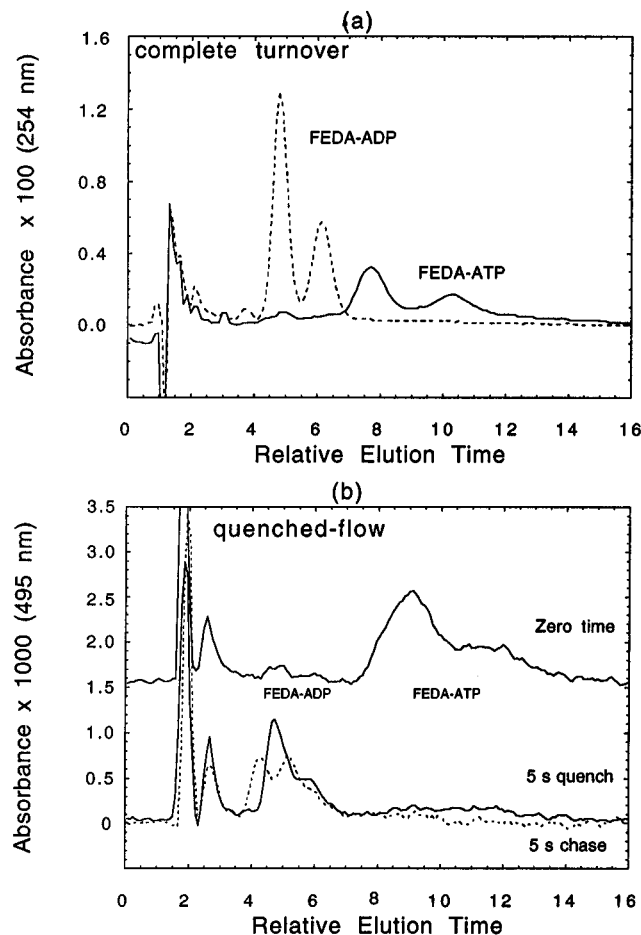


FIGURE 3: Hydrolysis of FEDA-ATP by S1 monitored by HPLC. (a) FEDA-ATP ( $75 \mu\text{M}$ ) was treated for 15 min with S1 ( $10 \mu\text{M}$ ) to convert it to FEDA-ADP. The reaction was quenched with 10% perchloric acid, the pH immediately readjusted to 4, and the denatured protein removed by centrifugation. The supernatant ( $20 \mu\text{L}$ ) was loaded onto a SAX column and eluted as described in the methods (---). Zero time control showing initial FEDA-ATP (—). The elution was monitored at 254 nm. Both FEDA-ADP and FEDA-ATP eluted as doublet peaks in a 2:1 ratio corresponding to the putative 3' and 2' isomers, respectively (see text). (b) Quenched-flow experiment to determine the state of the nucleotide during a single turnover of FEDA-ATP. Buffer conditions were as for Figure 1. Fifty micromolar S1 ( $120 \mu\text{L}$ ) was mixed with  $25 \mu\text{M}$  FEDA-ATP ( $120 \mu\text{L}$ ) (syringe concentrations), and the reaction was quenched in  $240 \mu\text{L}$  of 10% perchloric acid after 5 s, with the instrument operating in the double-push mode. The quenched mixture was immediately neutralized with NaOH and the denatured protein removed by centrifugation. The supernatant was analyzed by HPLC, showing that  $\geq 80\%$  of the nucleotide was present as the 2' and 3' isomers of FEDA-ADP (---). A similar reaction mixture was chased with  $500 \mu\text{M}$  ATP at 5 s and then the reaction quenched with perchloric acid after 60 s (---). A zero-time control, displaced vertically for clarity, is also shown (—). The elution was followed at 495 nm to avoid absorbance from the excess of ATP in the chase experiment. The initial sharp peak represents a refractive index change upon injection, while the subsequent peak(s) eluting before FEDA-ADP may represent free fluorescein or FEDA-AMP produced by breakdown of the nucleotide during quenching.

identified two peaks of comparable magnitude when we further chromatographed FEDA-ATP preparations on a Mono-Q ion-exchange column, which we attributed to these isomers (Sowerby et al., 1993). We achieved better separation of the di- and triphosphate positional isomers on an HPLC SAX column. FEDA-ATP gave two major peaks in about a 2:1 molar ratio (Figure 3a), suggesting that the first peak to elute is the 3' isomer. Addition of catalytic amounts

of S1 to the FEDA-ATP resulted in complete conversion to FEDA-ADP which retained a similar 2:1 ratio of isomers (Figure 3a). Thus, both isomers appeared to be substrates for the myosin ATPase, although from this experiment alone, it is possible that only one is actively hydrolyzed with spontaneous conversion occurring between isomers.

The SAX column allowed a small-scale preparation of the separate isomers. At pH 7, we detected no interconversion of the 2' and 3' FEDA-ATP after 24 h. The two peaks corresponding to the putative 2' and 3' FEDA-ATP were diluted immediately after elution from the column and mixed with a large excess of S1 in the stopped-flow apparatus. The fluorescence transients were similar for both isomers and indicated that the turnover rates were nearly identical ( $0.09\text{ s}^{-1}$  for the putative 2' isomer and  $0.07\text{ s}^{-1}$  for the putative 3' isomer). Previously, Woodward et al. (1991) studied the 2' deoxy mant-nucleotides and showed they had kinetics similar to those of the mixed 2',3' isomer preparation of conventional mant-nucleotides. For these reasons, we have used mixed-isomer preparations for most of our measurements.

**Hydrolysis of FEDA-ATP by S1.** To check whether ATP turnover was limited by phosphate release (step 3), as in the case of ATP itself, or the hydrolysis step (step 2), a quenched-flow experiment was performed. S1 was mixed with FEDA-ATP under single-turnover conditions, and the reaction mixture was acid-quenched after 5 s with the instrument operating in the double-push mode (Eccleston et al., 1985). At this time, the FEDA-ATP binding reaction is practically complete but very little product should be dissociated (cf. Figure 1a), so that the bound nucleotide is distributed between the  $\text{M}\cdot\text{FEDA-ATP}$  and  $\text{M}\cdot\text{FEDA-ADP}\cdot\text{P}_i$  states [cf. Bagshaw and Trentham (1973)]. HPLC analysis shows that  $\geq 80\%$  of the nucleotide was present as the 2' and 3' isomers of FEDA-ADP (Figure 3b). The remaining FEDA-ATP could be attributed to the  $\text{M}\cdot\text{FEDA-ATP}$  state or to nucleotide bound to other nonspecific sites. To distinguish between these possibilities, a similar reaction mixture was chased with  $500\text{ }\mu\text{M}$  ATP at 5 s and then acid-quenched after 60 s. Within the limits of the integration of the HPLC traces, the residual FEDA-ATP observed in the absence of ATP appeared largely hydrolyzed to FEDA-ADP in the presence of ATP (Figure 3b). This is in accord with an effectively irreversible FEDA-ATP binding step ( $k_{-1} \approx 0$ ) followed by a rapid but reversible hydrolysis step with an equilibrium constant,  $K_2$ , of  $\geq 4$ . Thus, the predominant steady-state intermediate is the  $\text{M}\cdot\text{FEDA-ADP}\cdot\text{P}_i$  complex. The HPLC profiles also confirm that both 2' and 3' isomers of FEDA-ATP are hydrolyzed rapidly by S1.

**FEDA-ADP Dissociation.** FEDA-ADP was generated by mixing FEDA-ATP with S1 in one syringe of the stopped-flow apparatus and allowing sufficient time for complete turnover. The FEDA-ADP dissociation rate constant ( $k_{+4}$ ) was then measured by displacement with excess ATP (Figure 4a). The reaction was accompanied by a biphasic increase in fluorescein fluorescence. The rate constants and relative amplitudes (in parentheses) of  $3.2\text{ s}^{-1}$  (0.43) and  $0.37\text{ s}^{-1}$  (0.67) were close to those for ADP displacement of  $4.5\text{ s}^{-1}$  (0.59) and  $0.37\text{ s}^{-1}$  (0.41) from the same S1 preparation measured by the change in tryptophan fluorescence (Figure 4b). Similar biphasic responses have been reported previously both for FEDA-ATP (Sowerby et al., 1993) and for mant-ATP (Woodward et al., 1991). The origin of the

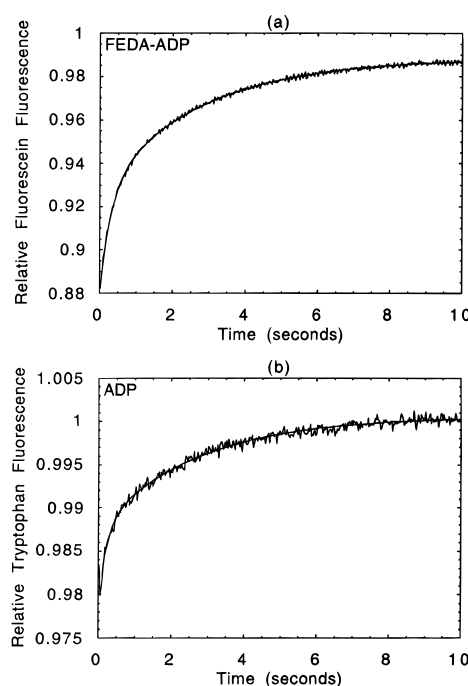


FIGURE 4: (a) FEDA-ADP release monitored by fluorescein fluorescence in the stopped-flow apparatus. FEDA-ATP ( $2\text{ }\mu\text{M}$ ) was mixed with S1 ( $10\text{ }\mu\text{M}$ ) in one of the drive syringes and preincubated for 5 min to allow complete turnover before pushing against ATP ( $100\text{ }\mu\text{M}$ ) (syringe concentrations). Buffer conditions were as for Figure 1. Fluorescence is shown normalized to the end point of the reaction. The line superimposed is the least-mean-squares double exponential fit having rate constants and relative amplitudes (in parentheses) of  $3.2\text{ s}^{-1}$  (0.43) and  $0.37\text{ s}^{-1}$  (0.67). The total amplitude suggests that the initial fluorescence is quenched by 11% of the fluorescence of free FEDA-ATP. (b) A parallel experiment in which ADP release is monitored by tryptophan fluorescence. S1 ( $1\text{ }\mu\text{M}$ ) was premixed with ADP ( $5\text{ }\mu\text{M}$ ) before pushing against  $50\text{ }\mu\text{M}$  ATP (syringe concentrations). Fitted rate constants and relative amplitudes (in parentheses) are  $4.5\text{ s}^{-1}$  (0.59) and  $0.37\text{ s}^{-1}$  (0.41).

biphasicity is not clear, but possibilities include a two-step nucleotide diphosphate-release mechanism or protein heterogeneity. Nevertheless, FEDA-ADP dissociation is at least an order of magnitude faster than the overall FEDA-ATP turnover, confirming that  $\text{M}\cdot\text{FEDA-ADP}\cdot\text{P}_i$  is the predominant steady-state intermediate. This is also consistent with the observed fluorescence quenching during multiple turnovers. There was no indication of a partial recovery following the binding phase which would be expected if a second process, such as FEDA-ADP release, contributed significantly to the overall steady-state flux [cf. Bagshaw and Trentham (1974)].

For REDA-ADP, the same procedure yielded rate constants and relative amplitudes (in parentheses) of  $1.8\text{ s}^{-1}$  (0.38) and  $0.31\text{ s}^{-1}$  (0.62). Thus, both ADP analogs mimic ADP to within a factor of 2 with regard to their dissociation rate constants.

**acto-S1 Dissociation by FEDA-ATP.** FEDA-ATP-induced dissociation of acto-S1 was monitored by light scattering in the stopped-flow apparatus (Figure 5a). The relative amplitude of the light-scattering transient observed with FEDA-ATP was essentially the same as that for ATP, monitored under the same conditions, suggesting that the extent of protein dissociation is similar. Under pseudo-first-order conditions with excess FEDA-ATP, the transients fitted well to single exponentials. The pseudo-first-order rate constant

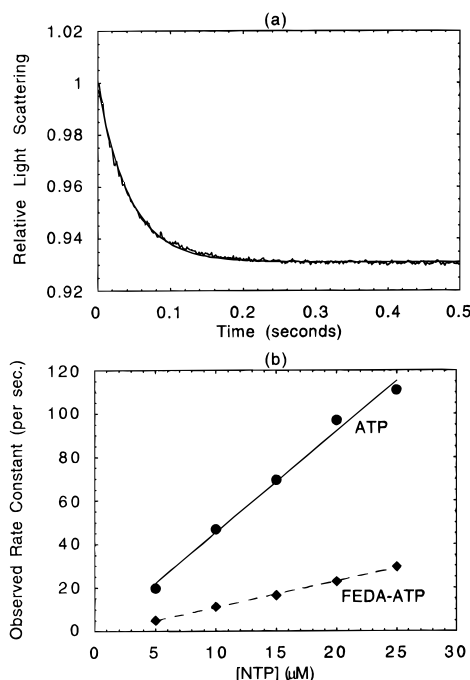


FIGURE 5: FEDA-ATP-induced dissociation of acto-S1. acto-S1 ( $1 \mu\text{M}$ ) was rapidly mixed with FEDA-ATP ( $20 \mu\text{M}$ ) in the stopped-flow apparatus and the reaction monitored by  $90^\circ$  light scattering at  $350 \text{ nm}$ . Buffer conditions were as for Figure 1. The transient is shown in a. The signal is shown normalized to the beginning of the reaction. The line superimposed is the least-mean-squares single exponential fit;  $k = 22.7 \text{ s}^{-1}$ . Part b shows the dependence of the pseudo-first-order rate constants on the concentration of FEDA-ATP ( $\blacklozenge$ ). Data obtained in a parallel experiment with ATP are shown for comparison ( $\bullet$ ). The data are shown fitted by linear regression with zero origin. The slopes are  $1.21 \times 10^6 \text{ M}^{-1} \text{ s}^{-1}$  for FEDA-ATP and  $4.66 \times 10^6 \text{ M}^{-1} \text{ s}^{-1}$  for ATP. Protein concentrations are  $1 \mu\text{M}$  actin and  $1 \mu\text{M}$  S1 for all data points.

varied in direct proportion with the concentration of FEDA-ATP (Figure 5b) with no indication of a definable saturation over the measurable range (which is limited by innerfilter effects attenuating the signal). The apparent second-order rate constant, given as the slope of these plots, is a factor of 4 slower for FEDA-ATP than for ATP ( $1.2 \times 10^6 \text{ M}^{-1} \text{ s}^{-1}$  for FEDA-ATP compared to  $4.7 \times 10^6 \text{ M}^{-1} \text{ s}^{-1}$  for ATP). Interestingly, the ratio of these values is similar to that found for NTP binding to S1 alone.

At  $>30 \mu\text{M}$  FEDA-ATP, the pseudo-first-order rate constants observed in the presence of actin increased further relative to those measured in the absence of actin owing to the saturation observed in the latter case. This may arise because the fluorescence change occurs on a relatively slow step which could occur after actin dissociation or because the process monitored by fluorescence is actin-activated. To distinguish these possibilities, the dissociation of  $10 \mu\text{M}$  acto-S1 induced by  $100 \mu\text{M}$  FEDA-ATP was monitored by light scattering, and fluorescein fluorescence of the same reaction mix was recorded in subsequent pushes of the stopped-flow apparatus. At these concentrations, protein dissociation was more than a factor of 2 faster than the transients observed in the absence of actin. The fluorescein fluorescence transient observed was essentially in phase with the light-scattering transient, suggesting that actin influences the process observed ( $k = 51 \text{ s}^{-1}$  for fluorescence,  $k = 57 \text{ s}^{-1}$  for light scattering). Unfortunately, the diminishing fluorescence signal prevented definition of the maximum rate

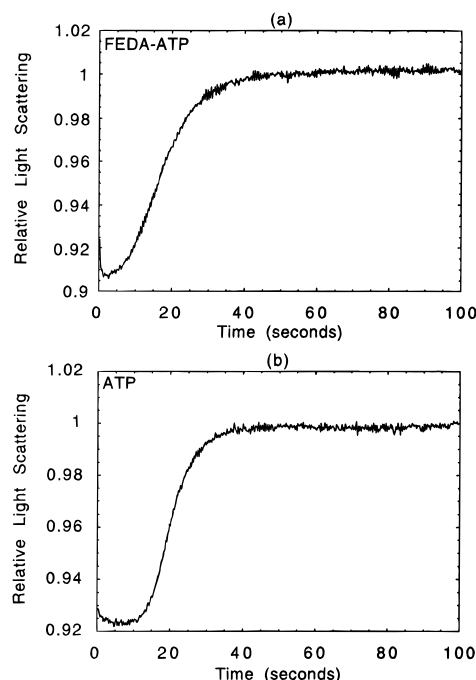


FIGURE 6: Actin-activated hydrolysis of FEDA-ATP measured by a limited-turnover experiment. (a) Actin ( $5 \mu\text{M}$ ) and S1 ( $1 \mu\text{M}$ ) were premixed and then pushed against FEDA-ATP ( $10 \mu\text{M}$ ) in the stopped-flow apparatus. The dissociation and reassociation of the proteins was monitored by  $90^\circ$  light scattering at  $320 \text{ nm}$ . Part b shows a parallel experiment with ATP. The signal is shown normalized to that observed at the end point of the reaction. Times to 50% recovery of the light scattering signal were 17 s for FEDA-ATP and 20 s for ATP. Buffer conditions were  $20 \text{ mM}$  Tes,  $1 \text{ mM}$   $\text{MgCl}_2$ , and  $\text{pH } 7.5$  at  $20^\circ \text{C}$  (approximately  $14 \text{ mM}$  ionic strength).

constant achieved in the presence of actin. The implications of this latter result are taken up in the Discussion.

Changes in light scattering were also used to measure the actin-activated ATPase (White & Taylor, 1976). Under conditions of a limited excess of NTP, the light-scattering signal remains low during the steady-state phase (because the proteins are largely dissociated) and returns to the initial value when the NTP is exhausted and the proteins reassociate (Figure 6). In a low-ionic strength buffer ( $14 \text{ mM}$ ), the time for turnover of  $10 \mu\text{M}$  NTP by  $1 \mu\text{M}$  S1 in the presence of  $5 \mu\text{M}$  actin yielded similar turnover rates for the two nucleotides ( $0.50$  and  $0.58 \text{ s}^{-1}$  for ATP and FEDA-ATP, respectively). These values represent a 7–8-fold activation over the turnover rates observed in the absence of actin under the same conditions.

**FEDA-ADP·AlF<sub>4</sub><sup>−</sup> and FEDA-ADP·BeF<sub>x</sub> Complexes.** Aluminum and beryllium fluorides are phosphate analogs which form stable trapped complexes analogous to the  $\text{M} \cdot \text{ADP} \cdot \text{P}_i$  (or  $\text{M} \cdot \text{ATP}$ ) state (Maruta et al., 1993; Fisher et al., 1995). Formation of the  $\text{M} \cdot \text{FEDA-ADP} \cdot \text{AlF}_4^-$  and  $\text{M} \cdot \text{FEDA-ADP} \cdot \text{BeF}_x$  complexes (where  $x$  represents a variable stoichiometry of fluorine atoms; Henry et al., 1993) was monitored from the quench in fluorescein fluorescence. In a typical experiment,  $1 \mu\text{M}$  FEDA-ATP was added to  $2 \mu\text{M}$  S1 to effect a single turnover (after which  $\text{M} \cdot \text{FEDA-ADP}$  is the predominant species).  $\text{NaF}$  ( $5 \text{ mM}$ ) was then added, followed by  $100 \mu\text{M}$   $\text{AlCl}_3$  or  $\text{BeCl}_2$ , and the fluorescence was monitored over several hours (Figure 7). Either narrow excitation slit widths ( $1 \text{ nm}$ ) or discontinuous illumination was used to minimize photodecomposition of the fluorescein. The time course fitted an exponential profile yielding rate constants

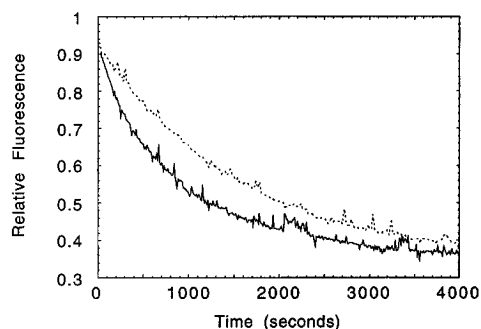


FIGURE 7: Formation of ternary complexes between S1-FEDA-ADP and  $\text{AlF}_4^-$  (···) and  $\text{BeF}_3^-$  (—) monitored by fluorescein fluorescence. S1 ( $2\ \mu\text{M}$ ) was initially mixed with FEDA-ATP ( $1\ \mu\text{M}$ ), and the reaction was followed for a few minutes to allow turnover of FEDA-ATP to FEDA-ADP (not shown). Ternary complex formation was initiated by addition of  $0.1\ \text{mM}$  aqueous  $\text{AlCl}_3$  (or  $\text{BeCl}_2$ ) and  $5.3\ \text{mM}$  NaF. Buffer conditions were  $20\ \text{mM}$  NaCl,  $10\ \text{mM}$  Tris,  $1\ \text{mM}$   $\text{MgCl}_2$ , and pH 7.5 at  $20\ ^\circ\text{C}$ . An excitation slit width of  $1\ \text{nm}$  was used to minimize photodecomposition. Analysis of the records yield rate constants of  $k = 5.2 \times 10^{-4}\ \text{s}^{-1}$  for  $\text{AlF}_4^-$  and  $k = 1.1 \times 10^{-3}\ \text{s}^{-1}$  for  $\text{BeF}_3^-$ . The final intensity of fluorescence represents 45% of that of the FEDA-ATP alone.

of  $5.2 \times 10^{-4}\ \text{s}^{-1}$  for  $\text{AlF}_4^-$  and  $1.1 \times 10^{-3}\ \text{s}^{-1}$  for  $\text{BeF}_3^-$ . These values are 5–10-fold slower than the corresponding values for trapping ADP at somewhat higher nucleotide concentrations (Maruta et al., 1993). The final fluorescence intensities were typically about 40–50% of that for the FEDA-ATP alone. In some experiments, the reaction mixture containing the trapped complex was passed through a gel-exclusion spin column (Wells & Bagshaw, 1985) to remove any unbound fluorophore. Sodium dodecyl sulfate (SDS) (1%) was then added to an aliquot of the eluant to release the trapped nucleotide, and the fluorescence change was measured. This showed that the fluorescence of the  $\text{M}\cdot\text{FEDA-ADP}\cdot\text{AlF}_4^-$  state was about 30% of that of free FEDA-ATP. Addition of excess ATP to the trapped  $\text{M}\cdot\text{FEDA-ADP}\cdot\text{AlF}_4^-$  complex resulted in less than 30% displacement after 20 h, indicating a product dissociation rate constant of less than  $5 \times 10^{-6}\ \text{s}^{-1}$ .

These long-lived product complexes allowed further spectroscopic characterization of the bound nucleotide. For the  $\text{M}\cdot\text{FEDA-ADP}\cdot\text{AlF}_4^-$  complex, there is a decrease in absorbance at  $495\ \text{nm}$ . This might be attributed to a shift in the  $pK$  of the xanthene group on binding to S1 such that the fluorescein monoanion or a neutral species (observed in solution at pH 5.5) is favored (Abdul-Halim, 1970). However, the reduction in the intensity of the absorption at  $495\ \text{nm}$  is not accompanied by any marked blue shift of the kind characteristic of these protonated species (Figure 8a). Likewise, the emission spectrum of the complex resembles a scaled-down dianion emission spectrum with little sign of shoulders above  $560$  and below  $490\ \text{nm}$ , as is observed for free FEDA-ATP at pH 5.5 (Figure 8b). Similar spectra were obtained with the  $\text{M}\cdot\text{FEDA-ADP}\cdot\text{BeF}_3^-$  complex. Therefore, FEDA-ATP binding to rabbit skeletal myosin S1 is accompanied by a decrease in total absorbance and a decrease in total fluorescence intensity rather than any marked spectral shifts. Comparison of the absorbance and fluorescence spectra suggests that part (approximately half) of the observed fluorescence quench can be attributed to the nonabsorbing state, though the remainder appears to result from a second state with a reduced quantum yield.

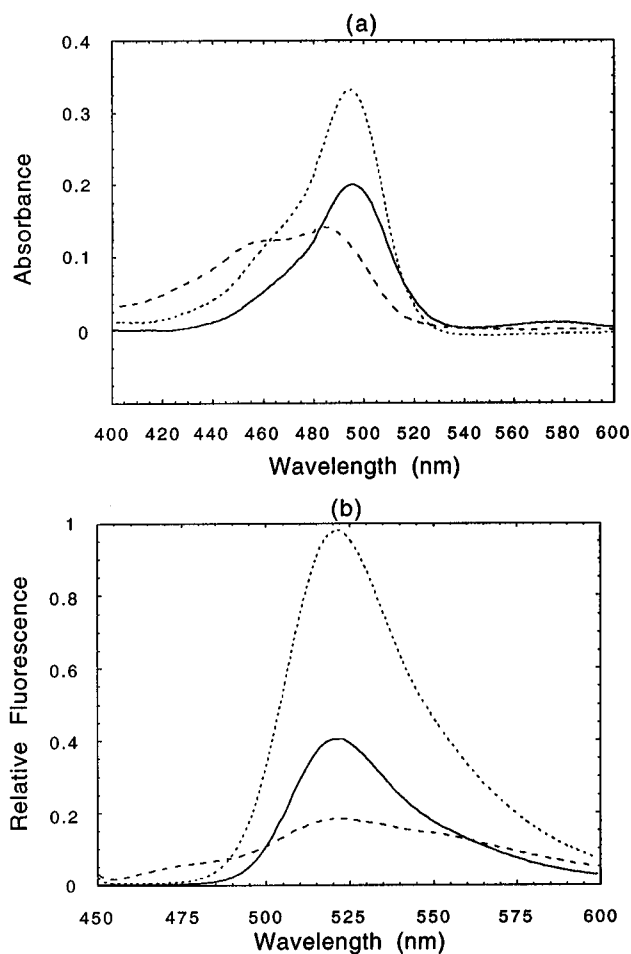


FIGURE 8: Absorption and fluorescence emission spectra of FEDA-ADP trapped as the  $\text{M}\cdot\text{ADP}\cdot\text{AlF}_4^-$  complex. (a) FEDA-ATP ( $4\ \mu\text{M}$ ) was reacted with S1 ( $8\ \mu\text{M}$ ), and the FEDA-ADP product was trapped as the  $\text{M}\cdot\text{FEDA-ADP}\cdot\text{AlF}_4^-$  complex as described in Figure 7. After 3 h, the absorption spectrum was measured (—). Then 1% SDS was added and the spectrum remeasured at pH 7.5 (···). A spectrum of FEDA-ATP at pH 5.5 is shown for comparison (---). (b) Uncorrected fluorescence emission spectra for the  $1\ \mu\text{M}$   $\text{M}\cdot\text{FEDA-ADP}\cdot\text{AlF}_4^-$  complex in the native state (—), after the addition of 1% SDS at pH 7.5 (···) and after adjustment of the pH to 5.5 (---). The excitation wavelength was  $436\ \text{nm}$ .

The fluorescence lifetime of the fluorescein moiety for free FEDA-ATP was measured as  $4.2\ \text{ns}$  at pH 7.0, in line with literature values for fluorescein itself (Lakowicz, 1983). Measurements on the  $\text{M}\cdot\text{FEDA-ADP}\cdot\text{AlF}_4^-$  complex reveal two spectroscopic states: one with a similar  $4.2\ \text{ns}$  component plus a second state with a shorter ( $1.1\ \text{ns}$ ) lifetime contributing 20% of the observed fluorescence signal. Assuming that the quantum yield of this second state is reduced in proportion to its lifetime by dynamic quenching, then the two observed states would be occupied in roughly equimolar proportions. Together, these states could account for a quench to 62.5% of the fluorescence of free FEDA-ATP. Comparison with the measured fluorescence intensity for the same preparation (41%) suggests that the bound nucleotide must actually comprise three fluorescein states in approximately equimolar proportions, with a significant amount of a nonfluorescent state which makes no contribution to the lifetime measurement.

Steady-state polarization measurements indicate that rotation of the fluorescein moiety becomes restricted upon formation of the  $\text{M}\cdot\text{FEDA-ADP}\cdot\text{AlF}_4^-$  complex, with the observed anisotropy value increasing from 0.046 for the free

FEDA-ATP (standard deviation of 0.002,  $n = 50$ ) to 0.126 (standard deviation of 0.003,  $n = 50$ ) for the trapped complex.

## DISCUSSION

The high absorption coefficients of fluorescein and rhodamine and their high quantum yields in the visible region have made them favored probes for fluorescence microscopy for many years. However, these fluorophores are relatively bulky compared with ATP so that fluorescent analogs incorporating these probes are likely to show perturbations in their interactions with ATPases and other nucleotide-utilizing enzymes. Fortunately, myosin has proven relatively unselective in substrate interactions, possibly because the active-site cleft is rather wide and many contacts with the nucleoside moiety are made through intervening water molecules (Fisher et al., 1995). These structural studies also indicate that the 2' and 3' ribose hydroxyl groups face the solvent and hence offer potential groups for derivatization with minimal effect on interactions. Overall, it seems reasonable that FEDA- and REDA-ATP should serve as satisfactory ATP analogs suitable for use in fluorescence microscopy.

Broadly speaking, this study confirms that FEDA-ATP is a satisfactory analog. Rate constants which control nucleotide turnover and product release show less than a factor of 2 difference compared with those of ATP. However, a larger (4-fold) difference between the two nucleotides was found when NTP binding to S1 and NTP-induced dissociation of acto-S1 were examined. Although simplified in Scheme 1, ATP is known to bind to S1 via a collision complex followed by at least one isomerization with the change in tryptophan fluorescence occurring on the isomerization step(s) and/or the hydrolysis step (Johnson & Taylor, 1978; Millar & Geeves, 1988). Similarly, ATP-induced dissociation of acto-S1 is known to involve ATP binding via a collision complex followed by a rate-limiting isomerization of the ternary complex and subsequent protein dissociation (Geeves, 1991). Analogous pathways may be envisaged for FEDA-ATP. The apparent second-order rate constants may therefore be a composite function of more than one rate constant, and the 4-fold difference observed may be the culmination of smaller effects on a number of steps. It is also pertinent to note that the fluorescence change occurring on binding FEDA-ATP may occur in response to local conformational changes in the vicinity of the fluorophore distinct from those monitored in the case of ATP and may even be controlled by the inherent properties of the fluorophore (e.g. a tautomerization step). This may also contribute to some of the difference in the apparent second-order rate constant.

For ATP binding to S1 alone, the observed rate constant for the protein fluorescence change reaches a limiting value at high concentrations (although no limiting rate is measurable for acto-S1). The maximum rate constant,  $k_{\max}$ , differs by a factor of 2 for ATP and FEDA-ATP, perhaps indicating that a step subsequent to initial binding is altered; however, since it need not be the case that  $k_{\max}$  is controlled by a common event for both nucleotides, this difference is difficult to interpret. It has been suggested that for ATP  $k_{\max}$  is controlled by the hydrolysis step (Johnson & Taylor, 1978; Millar & Geeves, 1988). For FEDA-ATP, however, this is

unlikely to be the case as the fluorescein fluorescence transient is apparently accelerated in the presence of actin while the hydrolysis step occurs after dissociation and has the same kinetics for acto-S1 and S1 alike. Thus, for FEDA-ATP, it is more likely to be controlled by a preceding event. Sowerby et al. (1993) suggested that  $k_{\max}$  was lower than that observed in the present work, but these earlier experiments were carried out at a lower protein-to-nucleotide ratio where the signal-to-noise ratio was reduced.

Any difference in nucleotide binding itself may reflect, in part, the reduced diffusion constant of FEDA-ATP which is about double the molecular mass of ATP. Another possible contributory factor is intramolecular association of the ATP analog. From the deviation of Beer's law, it is thought that fluorescein forms a dimer at high concentrations with an apparent dissociation constant of about 60 mM (Förster & König, 1957). Rhodamine shows an even greater tendency to dimerize with a  $K_d$  of around 0.5 mM (López Arbelo & Ojeda, 1981). While our studies have been conducted at much lower concentrations of fluorescent nucleotides, such interactions between aromatic rings suggest the possibility of intramolecular association between the adenosine and xanthene rings. Molecular dynamics simulations of the FEDA-ATP structure, using Insight II (Biosym Technologies), indicate that the most stable state of FEDA-ATP is a U-shaped conformation, with stacked aromatic rings, rather than an extended form. Given that FEDA-ATP would need to extend so that the adenosine moiety can fit into the active site (Fisher et al., 1995), such intramolecular association would effectively reduce the rate of FEDA-ATP binding.

*Comparison with Other Fluorescent ATP Analogs.* It is of interest to compare the properties of FEDA-ATP with other fluorescent ATP analogs that have been used to probe the actomyosin mechanism. mant-ATP shows apparent second-order association rate constants similar to those of ATP upon binding to skeletal S1 and acto-S1 (Woodward et al., 1991). The fluorescence transient reaches a maximum of about 80 s<sup>-1</sup>, whereupon it lags behind dissociation of acto-S1. This value is comparable to that observed with ATP and is consistent with limitation by the hydrolysis step. In these respects, mant-ATP is a better analog than FEDA-ATP, although mant-ADP release from S1 appears to be 10-fold slower than for ADP (Woodward et al., 1991).

With respect to adenine-modified analogs, the second-order rate constants for 1-*N*<sup>6</sup>-etheno-2-azaadenosine triphosphate binding to cardiac S1 and acto-S1 are 2–10-fold slower than for ATP and a significant component of the transient showed saturation at a rate 4-fold lower than for ATP (Smith & White, 1984). With 1-*N*<sup>6</sup>-ethenoadenosine triphosphate binding to skeletal S1, the hydrolysis step (measured directly) was much slower (5–10 s<sup>-1</sup>) than that for ATP and the equilibrium position favored the M•ATP state (Rosenfeld & Taylor, 1984). Both of these analogs with modified adenine rings showed a turnover rate with S1 alone that was approximately 2-fold higher than for ATP, while actin activation was limited to around 5-fold over the basal myosin ATPase rate (Rosenfeld & Taylor, 1984; White et al., 1993). In the case of FEDA-ATP, we have established that the M•ADP•P<sub>i</sub> state is the predominant steady-state intermediate and actin activation appears comparable to that observed with ATP.



It is likely that a variety of fluorophores could be introduced via a 2'/3' ethylenediamine linker without any marked changes in ATPase kinetics beyond those we have characterized for FEDA-ATP. Although we have carried out fewer measurements with other fluorophores, we have shown that the overall kinetics of interaction are similar for both REDA-ATP and Cy3-EDA-ATP. Also, we have introduced photoactivatable caged fluorescein in this manner and shown that the caged FEDA-ATP is a substrate for myosin (Jeffreys et al., 1995).

Recently, Funatsu et al. (1995a) demonstrated the advantageous photochemical characteristics of the cyanine dyes, Cy3 and Cy5, for single-molecule detection by fluorescence microscopy. The Cy3-based ATP analog first used by these authors was derivatized through the N<sup>6</sup>-position of the adenine ring. The effect of this modification on the ATPase mechanism was not characterized in detail, although as noted above, myosin is much less tolerant of modifications of the adenine ring than of modifications of the ribose moiety. The finding here that Cy3-EDA-ATP is a reasonable analog suggests that it could be used to possible advantage in single-molecule studies. Indeed, in more recent single-molecule studies, these investigators have chosen to use Cy3-EDA-ATP as a probe (Saito et al., 1995). The enhancement of fluorescence upon the binding of this analog to S1 in solution contrasts with the quenching of fluorescence for FEDA-ATP and REDA-ATP and should result in about a 2-fold gain in contrast in microscopy measurements. Recently, Oiwa et al. (1995) have reported that Cy5-EDA-ATP is a substrate for the myosin and actomyosin ATPase with kinetics comparable to those found for FEDA-ATP.

It is also of interest to note that mant-ATP is a reasonable analog for the kinesin ATPase (Sadhu & Taylor, 1992). Thus, it is likely that 2'/3' ethylenediamine derivatives will also function satisfactorily in this microtubule-activated system. Preliminary studies show FEDA-ATP binding to kinesin is accompanied by a small quench in fluorescence (R. A. Cross, personal communication), while Cy3-EDA-ATP has been used to investigate single-molecule turnover by kinesin (Funatsu et al., 1995b).

The ultimate test of an ATP analog is its ability to support contraction in muscle fibers. In this regard, it is pertinent to note that FEDA-ATP at a concentration as low as 10  $\mu$ M is sufficient to cause a single myofibril to contract auxotonically against a flexible glass needle (S. Chaen, I. Shirakawa, H. Sugi, and C. R. Bagshaw, unpublished observations).

**Origin of the Fluorescence Quench.** Fluorescein in free solution exists in multiple chemical (and hence spectroscopic) ionization states and tautomers. At low pH, a complex mixture of states prevails, while above pH 7, the highly fluorescent dianion predominates. The neutral and monoanion forms of fluorescein have lower absorbancies, and their quantum yields are between one-third and one-fifth of that of the dianion; the lactone tautomer is nonabsorbing, and hence nonfluorescent at visible wavelengths (Martin & Lindqvist, 1975). Comparison of the absorption and emission spectra (Figure 8) suggests that part (approximately half) of the fluorescence quench observed when FEDA-nucleotide binds to S1 can be attributed to reduced absorbance, while the remainder appears to result from a reduced quantum yield. The lifetime measurements are consistent with approximately equimolar proportions of a nonfluorescent state,

a dynamically quenched state with a 4-fold reduction in lifetime and quantum yield, and an unperturbed bound state (gel-exclusion chromatography indicates that only 11% of the nucleotide was unbound). This scenario is consistent with the spectral data, assuming that the nonfluorescent state is also nonabsorbing and the dynamically quenched state has an absorbance similar to that of free FEDA-ATP. The perturbation of the ground-state species leading to reduced or zero absorbance could reflect the stacking of fluorophore with surface aromatic residues on the protein, which would be consistent with the observed concomitant quench in tryptophan fluorescence and the increase in anisotropy. Alternatively, it is possible that the binding site may favor the nonabsorbing lactone tautomer of fluorescein. In any event, the lack of any change in spectral shape when FEDA-nucleotides bind to S1 clearly indicates that a local perturbation of the pK of the xanthene ring is not the main contributory factor. This proposal is in accord, also, with the comparable fluorescence quench observed upon binding REDA-ATP, which has tertiary/quaternary diethylamino groups in place of the hydroxyl groups of fluorescein. Moreover, the lactone form of rhodamine is predominant in nonpolar solvents (Hinckley et al., 1986) and therefore may be favored in certain protein binding sites.

In the case of mant- and DEDA-nucleotides, the fluorescence emission is enhanced about 2-fold and the fluorescence lifetimes are extended 2-fold upon binding to S1 (Cremo et al., 1990). We show here that Cy3-EDA-ATP also gives an enhancement upon binding S1. It therefore appears that these fluorophores are protected from some form of collisional quenching by the solvent. Indeed, Stern-Volmer plots suggest that bound mant-ADP is relatively inaccessible to further quenching by added acrylamide (Franks-Skiba & Cooke, 1995). DEDA-nucleotides show no evidence for further protection from added quenching agents once bound to S1 (Cremo et al., 1990). Although FEDA-, DEDA-, and Cy3-EDA-nucleotides have the same linking ethylenediamine chain and hence the fluorophores could experience the same environment, the relatively low quantum yield of the free dansyl and Cy3 groups (0.09 and 0.15, respectively) gives the potential for the binding process to protect against collision from water molecules. The fluorescein dianion, however, shows a large quantum yield in aqueous solution (>0.9; Martin & Lindqvist, 1975), and thus, there is little potential for further enhancement. On the other hand, there are several mechanisms by which the fluorescein fluorescence may be quenched, as noted above.

Whether a perturbation of fluorescence is observed at all appears to depend on rather specific interactions on the protein surface. Thus, in contrast to rabbit skeletal myosin, FEDA-ATP binding and turnover by scallop adductor myosin is accompanied by little change in fluorescein fluorescence. Nevertheless, it appears to be a reasonable substrate (Sowerby et al., 1993). The quenches and enhancements observed here are therefore fortuitous. However, they have revealed some aspects of the mechanism of interaction between 2'/3' ethylenediamine-linked ATP derivatives and the myosin and actomyosin ATPase and demonstrate their efficacy as ATP analogs.

## ACKNOWLEDGMENT

We thank M. Lee (Chemistry Department) for the synthesis of EDA-ATP.

## REFERENCES

- Abdel-Halim, F. M., Issa, R. M., El-Ezaby, M. S., & Hasanein, A. A. (1970) *Z. Phys. Chem. (Munich)* 73, 59–67.
- Bagshaw, C. R., & Trentham, D. R. (1973) *Biochem. J.* 133, 323–328.
- Bagshaw, C. R., & Trentham, D. R. (1974) *Biochem. J.* 141, 331–349.
- Bagshaw, C. R., Eccleston, J. F., Trentham, D. R., Yates, D. W., & Goody, R. S. (1972) *Cold Spring Harbor Symp. Quant. Biol.* 37, 127–135.
- Bagshaw, C. R., Matuska, M., & Spudich, J. A. (1992) *J. Muscle Res. Cell Motil.* 13, 266–267.
- Burton, K. (1992) *J. Muscle Res. Cell Motil.* 13, 590–607.
- Conibear, P. B., Seehra, C. K., Bagshaw, C. R., & Gingell, D. (1995) *Biochem. Soc. Trans.* 23, 400S.
- Cremo, C. R., Neuron, J. M., & Yount, R. G. (1990) *Biochemistry* 29, 3309–3319.
- Diehl, H., & Horchak-Morris, N. (1987) *Talanta* 34, 739–741.
- Eccleston, J. F., Dix, D. B., & Thompson, R. C. (1985) *J. Biol. Chem.* 260, 16237–16241.
- Ellis, J., Bagshaw, C. R., & Shaw, W. V. (1995) *Biochemistry* 34, 3513–3520.
- Finer, J. T., Simmons, R. M., & Spudich, J. A. (1994) *Nature (London)* 368, 113–119.
- Fisher, A. J., Smith, C. A., Thoden, J., Smith, R., Sutoh, K., Holden, H. M., & Rayment, I. (1995) *Biophys. J.* 68, 19s–28s.
- Förster, T. H., & König, E. (1957) *Z. Electrochem.* 61, 344–348.
- Franks-Skiba, K., & Cooke, R. (1995) *Biophys. J.* 68, 142s–149s.
- Funatsu, T., Harada, Y., Tokunaga, M., Saito, K., & Yanagida, T. (1995a) *Nature (London)* 374, 555–559.
- Funatsu, T., Higuchi, H., & Tokunaga, M. (1995b) *Biophysics (Toyonaka, Jpn.)* 35, S183.
- Garland, F., & Cheung, H. C. (1979) *Biochemistry* 18, 5281–5289.
- Geeves, M. A. (1991) *Biochem. J.* 274, 1–14.
- Harada, Y., Sakurada, K., Aoki, T., Thomas, D. D., & Yanagida, T. (1990) *J. Mol. Biol.* 216, 49–68.
- Hayashi, H., Takiguchi, K., & Higashi-Fujime (1989) *J. Biochem. (Tokyo)* 105, 875–877.
- Henry, G. D., Maruta, S., Ikebe, M., & Sykes, B. D. (1993) *Biochemistry* 32, 10451–10456.
- Hinckley, D. A., Seybold, P. G., & Boris, D. P. (1986) *Spectrochim. Acta* 42A, 747–754.
- Hiratsuka, T. (1983) *Biochem. Biophys. Acta* 742, 496–508.
- Jeffreys, D. S., Eaton, R. J., & Bagshaw, C. R. (1995) *Biochem. Soc. Trans.* 23, 401S.
- Johnson, K. A., & Taylor, E. W. (1978) *Biochemistry* 17, 3432–3442.
- Kishino, A., & Yanagida, T. (1988) *Nature (London)* 334, 74–76.
- Kron, S. J., & Spudich, J. A. (1986) *Proc. Natl. Acad. Sci. U.S.A.* 83, 6272–6276.
- Kron, S. J., Toyoshima, Y. Y., Uyeda, T. Q. P., & Spudich, J. A. (1991) *Methods Enzymol.* 196, 399–416.
- Lakowicz, J. R. (1983) *Principles of fluorescence spectroscopy*, Plenum Press, New York and London.
- Lopez Arbelo, I., & Ojeda, P. R. (1981) *Phys. Lett.* 79, 347–350.
- Margossian, S. S., & Lowey, S. (1982) *Methods Enzymol.* 85, 55–71.
- Martin, M. M., & Lindqvist, L. (1975) *J. Lumin.* 10, 381–390.
- Maruta, S., Henry, G. D., Sykes, B. D., & Ikebe, M. (1993) *J. Biol. Chem.* 268, 7093–7100.
- Millar, N. C., & Geeves, M. A. (1988) *Biochem. J.* 249, 735–743.
- Oiwa, K., Eccleston, J. F., Corrie, J. E. T., Anson, M., Yamada, A., Trentham, D. R., & Nakayama, H. (1995) *Biophysics (Toyonaka, Jpn.)* 35, S208.
- Rosenfeld, S. S., & Taylor, E. W. (1984) *J. Biol. Chem.* 259, 11920–11929.
- Sadhu, A., & Taylor, E. W. (1992) *J. Biol. Chem.* 267, 11352–11359.
- Saito, K., Tokunaga, M., Yokota, H., & Yanagida, T. (1995) *Biophysics (Toyonaka, Jpn.)* 35, S208.
- Smith, S. J., & White, H. D. (1985) *J. Biol. Chem.* 260, 15146–15155.
- Sowerby, A. J., Seehra, C. K., Lee, M., & Bagshaw, C. R. (1993) *J. Mol. Biol.* 234, 114–123.
- Tonomura, Y., Imamura, K., Ikehara, M., Uno, H., & Harada, F. (1967) *J. Biochem. (Tokyo)* 61, 460–472.
- Trentham, D. R., Eccleston, J. F., & Bagshaw, C. R. (1976) *Q. Rev. Biophys.* 9, 217–281.
- Uyeda, T. Q. P., Kron, S. J., & Spudich, J. A. (1990) *J. Mol. Biol.* 214, 699–710.
- Weeds, A. G., & Taylor, R. S. (1975) *Nature (London)* 257, 54–56.
- Wells, C., & Bagshaw, C. R. (1985) *Nature (London)* 313, 696–697.
- White, H. D., & Taylor, E. W. (1976) *Biochemistry* 15, 5818–5826.
- White, H. D., Belknap, B., & Jiang, W. (1993) *J. Biol. Chem.* 268, 10039–10045.
- Woodward, S. K. A., Eccleston, J. F., & Geeves, M. A. (1991) *Biochemistry* 30, 422–430.
- Yount, R. G. (1975) *Adv. Enzymol.* 43, 1–6.

BI951824+